Channel Correlation and Stationarity in mm-wave V2V Channels

Joseph Hoellinger [1], Gloria Makhoul [2], Raffaele D'Errico [3], Thierry Marsault [4]
[1]CEA-Leti, Univ. Grenoble Alpes Grenoble, France, joseph.hoellinger@cea.fr
[2]CEA-Leti, Univ. Grenoble Alpes Grenoble, Grenoble, France, gloria.makhoul@cea.fr
[3]CEA-Leti, Univ. Grenoble Alpes Grenoble, Grenoble, France, raffaele.derrico@cea.fr
[4]DGA-MI , Bruz, France, thierry.marsault@intradef.gouv.fr

***Abstract*—This paper investigates different methods to estimate the channel correlation properties over time for millimeter wave (mm-Wave) vehicle-to-vehicle (V2V) channels. The proposed metrics are applied on three V2V scenarios measured at 26 GHz. The correlation properties are derived from the Power Delay Profile (PDP) and the Local Scattering Function (LSF). The results are then analyzed in terms of quasi-stationary time intervals obtained from each approach.**

***Index Terms*—V2V, Measurement, Channel, Stationary-region, Correlation, Local Scattering Function.**

I. Introduction

The recent interest in autonomous driving vehicles and the rising demand in embedded infotainment such as video streaming will increase the demand for high speed vehicle to vehicle (V2V) data connection [1]. The main challenge to achieve such connection is having access to a large bandwidth which is only possible using millimeter wave (mm-waves) as the current V2V band around 5 GHz only allocates a view MHz to V2V communication. Therefore in the last few year the Ka band has been investigated for V2V communication [2].

A well-known issue in V2V, and more in general mobile-to-mobile channels, is the stationarity over time. A channel is considered stationary when its first and second order statistical moments are independent of absolute time of observation [3] . Classically, mobile channels are time dependent and the channel statistics are valid for a given time interval, i.e. the quasi-stationary region. The stationary region is usually identified by means of temporal correlation a certain threshold, e.g. 0.7, 0.8 and 0.9 [4]. However in literature different metrics have been considered, which could yield to different conclusions. In [5] the quasi-stationary region is evaluated for V2I scenarios at 1.9 GHz based on the temporal correlation coefficient. Using the same method, the quasi-stationary regions were determined for V2I and V2V at 5.9 GHz in [6]. The Local Scattering Function (LSF) collinearity can be also considered to evaluate the correlation properties in both time and frequency, as done in [7] for V2V highway and urban scenarios at 5.2 GHz. Also based on the LSF, results were presented at a frequency of 5.2 GHz for various V2V scenario (rural, tunnel, road crossing, bridge) in [8]. In [9] another method based on the analysis of the small scale fading correlation properties is presented for V2V measurement in the same frequency range. Few articles were studying mm-wave for V2V communication such as [10] where the correlation properties are evaluated based on the Pearson coefficient metric for V2V measurements at 60 GHz. At mm-waves the correlation properties are presented in [14] for V2V crossing and same direction same scenario. The main objective of this work is to evaluate the different metrics and evaluate them by means of measurements results in order to quantify the quasi-stationary regions of V2V channels. The paper is organized as follows: sec. II presents the mm-wave V2V channel measurement campaign for three different scenarios and mobility conditions; sec. III presents the different metrics considered and results shown in sec. IV. Finally sec. V concludes the paper.

II. Measurement campaign

Mm-Wave V2V channel measurements were conducted using real time channel sounder in order to record the time-varying channel impulse responses (CIRs). The channel sounder consists of two units, i.e. transmitter (Tx) and receiver (Rx) subsystems. Each of the two units was embarked in a van. Monopole antennas with 1.5 dBi gain were mounted on the roof of vans at a height of 2.1 m. The center frequency was 26 GHz with a bandwidth of 1 GHz resulting in a time delay resolution of 1 ns. A code length of 2047 ns was used which corresponds to a maximal theoretical measurement distance of 614.4 m. The time between two consecutive acquisitions was set to 80 µs, allowing a maximum Doppler frequency of 6.25 KHz. The measurement time was set to 20 s enabling a recording of 250 000 CIR for each scenario.
The measurement were conducted in different types of environments: Street canyon (Fig. 1a), Suburban environment (Fig. 3a) and Building obstruction (Fig. 5a).

III. Data processing

A. Power delay profile

From the measured CIR $h(t,\tau)$ we derive the time-variant PDP $h'_m(t,\tau)$ by averaging over N consecutive acquisitions spaced by Δt:

$$h'_m(t,\tau) = \frac{1}{N}\sum_{n=0}^{N-1} |h(n\Delta t,\tau)|^2 \quad (1)$$

By doing this operation, the small-scale fading is mitigated. The averaging factor N, is here considered to match a window of 15λ, based on average speed, in order to compare with previous results in literature [5]. Considering these parameters the averaging time window is set to 3.1 ms.

B. Local scattering function (LSF)

The LSF is used to obtain a channel description as function of the time t, the delay τ, the frequency f and the Doppler frequency ν. To calculate the LSF, first $H(t,f)$ is calculated using the Fourier transformation of the CIR $h(t,\tau)$. The channel cross correlation function RL is then derived using equation (2) as detailed in [11] .

$$RL(t,f,\Delta t,\Delta f) = \iint [H(t,f+\Delta f)\cdot H(t-\Delta t,f)]d\Delta t d\Delta f \tag{2}$$

From the channel cross correlation function the local scattering function is obtained from (3).

$$LSF(t,f,\tau,\nu) = RL(t,f,\Delta t,\Delta f)e^{-j2\omega(\nu\Delta t-\tau\Delta f)}d\Delta t d\Delta f \tag{3}$$

For our measurement campaign we calculate the local scattering function with a frequency interval $\Delta f = 15.6\,MHz$ and a time interval $\Delta t = 8ms$.

IV. Metrics

A. Pearson correlation coefficient (PCC)

Using the Pearson correlation coefficient from (4) with $\mu_{h'm}$ the mean value of the PDP h'_m and σ_{hm} the standard deviation. With this metric two PDPs at different time intervals t_1 and t_2 are compared regarding their energy distribution over the delay. The Pearson coefficient was used in [10] to estimate the correlation as function of the time lag Δt.

$$\rho(t_1,t_2) = \frac{\mathbb{E}[(h'_m(t_1,\tau)-\mu_{h'm\tau(t1)})(h'_m(t_2,\tau)-\mu_{h'm\tau(t2)})]}{\sigma_{h'm\tau(t1)}\sigma_{h'm\tau(t2)}} \tag{4}$$

B. Temporal PDP correlation coefficient (TPCC)

The temporal correlation coefficient was introduced in [5] for V2I measurement. This method evaluates the similarity in terms of energy from two PDP at fixed delay and different times instant similarly to PC. However compared to the PC, the TPCC is normalized by the PDP holding the most total energy as detailed in (5) and not the mean and standard deviation.

$$\rho(t_1,t_2) = \frac{\int h'_m(t_1,\tau)\cdot h'_m(t_2,\tau)\,d\tau}{\max\left(\int h'_m(t_1,\tau)^2\,d\tau, \int h'_m(t_2,\tau)^2\,d\tau\right)} \tag{5}$$

C. Cross correlation coefficient (CCC)

Where TPCC and PCC metric only calculate the correlation coefficient by comparing the energy at fixed delay positions, the CCC is based on the cross correlation of two PDP at different time instant as detailed in (6). This offers the possibility to compare PDP based on the shape of their energy distribution.

$$\rho(t_1,t_2) = \max_{\Delta\tau} \frac{\int h'_m(t_1,\tau)\cdot h'_m(t_2,\tau+\Delta\tau)\,d\tau}{\sqrt{\int h'_m(t_1,\tau)^2\,d\tau, \int h'_m(t_2,\tau)^2\,d\tau}} \tag{6}$$

D. Local Scattering Function Correlation Coefficient (LSFCC)

Previous metrics are applied on PDP, in this section, the correlation properties are derived using the LSFs which depend on the measured frequency, Doppler frequency, delay and time, as follows:

$$C(t,f,\tau,\nu) = |L_{SF}((t,f,\tau,\nu)|^2 \tag{7}$$

$$\rho_L(t_1,t_2) = \frac{\sum_{n=0}^{N_\tau}\sum_{n=-Nt/2}^{N_t/2-1}\sum_{n=-N_f/2}^{N_f/2-1} C(t_1,f,\tau,\nu)\odot C(t_2,f,\tau,\nu)}{||C(t_1)||_2\cdot||C(t_2)||_2} \tag{8}$$

This metric was used for different V2V measurement and is detailed in [8]. The energy C (7), of the two LSFs at t_1 and t_2 is multiplied element-wise product over the delay τ, Doppler frequency ν and the measured frequency f and then added. The LSFCC is scaled down using the product of the Froebius norm of the two LSF at fixed time instant as detailed in (8).

V. Results

A. Street canyon scenario

Fig. 1, shows the street canyon scenario with (a) the environment and (b) the PDP.

(a) Environment street canyon scenario

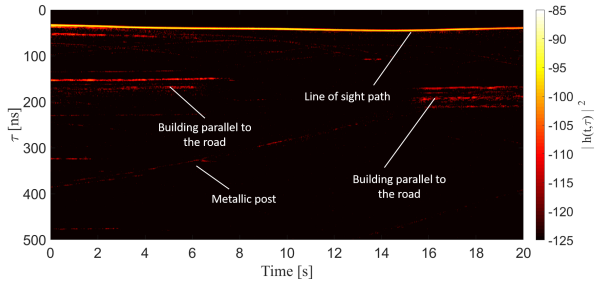

(b) PDP

Fig. 1: Street canyon scenario

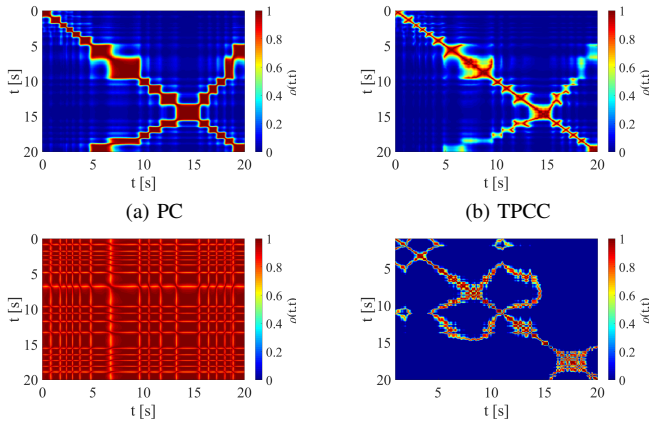

(a) PC (b) TPCC

(c) CCC (d) LSFCC

Fig. 2: Correlation properties street canyon scenario

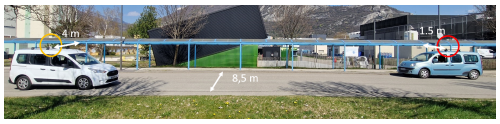

(a) Environment crossing scenario

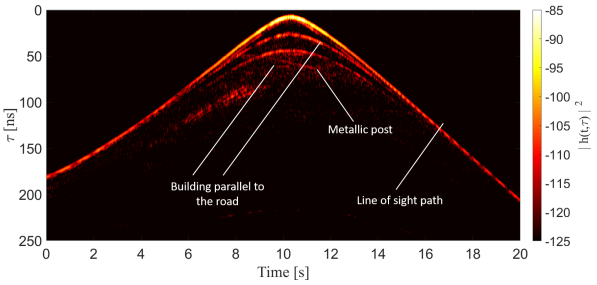

(b) PDP

Fig. 3: Crossing scenario

Fig. 2 shows correlation properties derived from the street canyon scenario. We note a strong shape similarity regarding the correlation properties between the PC (a) and the TPCC (b). However the correlation values are higher using the PC method while covering the same region as the TPCC method. For both TPCC and PC we also have a second correlation zone from 5 s to 20 s caused by some symmetry in the PDP. Using the CCC method (c) the correlation coefficients are always greater than 0.6 throughout the measurement duration. A high correlation is expected because the shape of the power delay profile is barely changing during the scenario as only the delay is slightly varying and some MPCs are changing over time. However we still observe some smaller region visible around the diagonal line, these are matching the region observe with TPCC and PC method. The LSFCC (d) results are differing from the three other methods as the Doppler frequency correlation is also evaluated in this method. We note that the highly correlated region with the CCC methods matches a time period were the delay, thus the distance between vehicles is constant, meaning constant speed and no Doppler frequency shift.

B. Crossing scenario

Fig. 3, shows the crossing scenario with (a) the environment and (b) the PDP.

When comparing correlation properties for the crossing scenario in Fig. 4 strong similarity between the PC (a) and the TPCC (b) is still present. In fact, with both of these methods the channel is mostly uncorrelated due to the relative mobility of both vehicles. Note that the second correlated zone forming a cross like shape is caused by the symmetry of the PDP between the first 10 s and last 10 s. Using the CCC (c) method, we observe a high correlation during the whole measurement. However the average correlation coefficient is lower than in the previous scenario. The LSFCC (d) method is showing a low correlation properties for the crossing scenario as both Doppler frequency is strongly varying over time in this scenario.

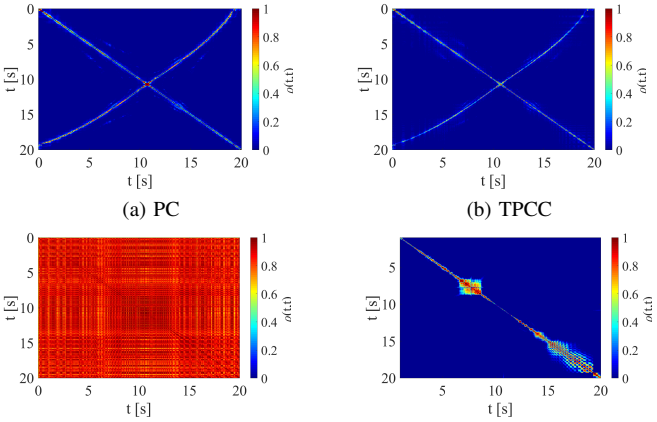

(a) PC (b) TPCC

(c) CCC (d) LSFCC

Fig. 4: Crossing scenario correlation properties

C. Building obstruction scenario

Fig. 5, shows the building obstruction scenario with (a) the environment and (b) the PDP.

(a) Environment building obstruction scenario

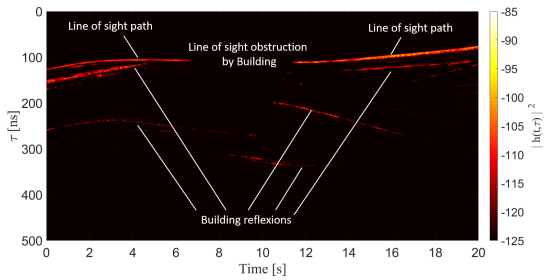

(b) PDP

Fig. 5: Building obstruction scenario

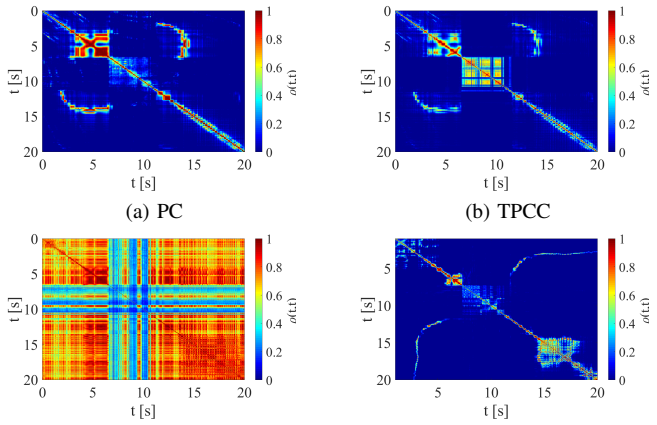

(a) PC (b) TPCC

(c) CCC (d) LSFCC

Fig. 6: Building obstruction scenario correlation properties

For the building obstruction scenario in Fig. 6, the TPCC (a) and PC (b) methods both show one strong correlation zone around 5 seconds. A second zone corresponding to the obstruction period is also visible using the TPCC (a) but barely with PC (b). The CCC (c) methods shows 3 distinct regions, the first one before 6 seconds corresponding to instants prior to the obstruction were the correlation is relatively strong ($\rho > 0.6$). The second one is located from 6 to 10 seconds corresponding to the obstruction time therefore having a low correlation coefficient ($\rho < 0.3$). The third one after 10 seconds when both Tx and Tx are back in LOS with strong correlation($\rho > 0.6$). The LSFCC (d) methods still shows weak correlation results except for few periods right before and after obstruction.

TABLE I: Comparing quasi-stationary time results in [s] for each scenario and each methods for $\rho = 0.7$

	Scenario 1		**Scenario 2**		**Scenario 3**	
	Mean	**Std**	**Mean**	**Std**	**Mean**	**Std**
PC	1,51	0,79	0,06	0,04	0,29	0,37
CCC	0,70	0,45	0,04	0,01	0,13	0,14
LSFCC	19,46	2,09	14,64	6,07	1,15	1,33
PC	0,18	0,11	0,13	0,14	0,10	0,10

From correlation properties we derive the quasi-stationary time by identifying the regions were the correlation coefficients are above a threshold of 0.7. Tab. I summarized for each method and for the three scenario the mean and the std of the quasi-stationary region. We note that the LSFCC always estimates the lower quasi stationary region, followed by the TPCC and PC methods and the CCC.

VI. Conclusion

In this article, we presented different methods to estimate the channel correlation properties and the quasi-stationary time: the PC, TPCC, CCC and LSFCC methods. The different methods were applied on three V2V scenarios: a following scenario, a crossing and a building obstruction. The outcome of each method for each scenario were compared and discussed based on the statistics of the quasi-stationary time obtained. As conclusion, we determined that the PCC and TPCC methods are relatively similar, as expected. In terms of shape of the correlation zone the two methods are almost identical but the PC methods return higher correlation than the TPCC. However those metrics could have limited information, since any scenario including relative mobility will results being weakly correlated. The CCC methods leads to comparing the shape of the PDP without considering the absolute time of arrival. Therefore this methods seems more relevant than the PC and TPCC for mobile channel as a stationary region is defined by its statistics and relative mobility doesn't necessary mean the channel is not-stationary. Finally the LSFCC method shows interesting applications as it estimates the energy distribution over several parameter such as delay, Doppler and frequency. However using the LSFCC metric as presented in this paper is affected by Doppler frequency variation and energy distribution over delay changes, which would result into low correlation for speed variation.

References

[1] T. S. Rappaport et al., "Millimeter Wave Mobile Communications for 5G Cellular: It Will Work!," in IEEE Access, vol. 1, pp. 335-349, 2013.

[2] W. Zheng, A. Ali, N. González-Prelcic, R. W. Heath, A. Klautau and E. M. Pari, "5G V2X communication at millimeter wave: rate maps and use cases," 2020 IEEE 91st Vehicular Technology Conference (VTC2020-Spring), 2020, pp. 1-5, doi: 10.1109/VTC2020-Spring48590.2020.9128612.

[3] G. Matz, "On non-WSSUS wireless fading channels," in IEEE Transactions on Wireless Communications, vol. 4, no. 5, pp. 2465-2478, Sept. 2005, doi: 10.1109/TWC.2005.853905.

[4] D. Czaniera et al., "Investigation on Stationarity of V2V Channels in a Highway Scenario," 2019 13th European Conference on Antennas and Propagation (EuCAP), 2019, pp. 1-5.

[5] Gehring, M. Steinbauer, I. Gaspard, and M. Grigat, "Empirical channel stationarity in urban environments," in Proc. Eur. Personal Mobile Communications Conf. (EPMCC), Vienna, Austria, February 2001.

[6] Z. Su et al., "Analysis of Channel Non-Stationarity for V2V and V2I Communications at 5.9GHz in Urban Scenarios," 2022 IEEE International Conference on Communications Workshops (ICC Workshops), 2022, pp. 1130-1134, doi: 10.1109/ICCWorkshops53468.2022.9814640.

[7] Paier et al., "Non-WSSUS vehicular channel characterization in highway and urban scenarios at 5.2GHz using the local scattering function," 2008 International ITG Workshop on Smart Antennas, 2008, pp. 9-15, doi: 10.1109/WSA.2008.4475530.

[8] L. Bernadó, T. Zemen, F. Tufvesson, A. F. Molisch and C. F. Mecklenbräuker, "The (in-) validity of the WSSUS assumption in vehicular radio channels," 2012 IEEE 23rd International Symposium on Personal, Indoor and Mobile Radio Communications - (PIMRC), 2012, pp. 1757-1762, doi: 10.1109/PIMRC.2012.6362634.

[9] R. He et al., "Characterization of Quasi-Stationarity Regions for Vehicle-to-Vehicle Radio Channels," in IEEE Transactions on Antennas and Propagation, vol. 63, no. 5, pp. 2237-2251, May 2015, doi: 10.1109/TAP.2015.2402291.

[10] J. Blumenstein et al., "Vehicle-to-Vehicle Millimeter-Wave Channel Measurements at 56-64 GHz," 2019 IEEE 90th Vehicular Technology Conference (VTC2019-Fall), 2019, pp. 1-5, doi: 10.1109/VTC-Fall.2019.8891543.

[11] G. Matz, "Doubly underspread non-WSSUS channels: analysis and estimation of channel statistics," 2003 4th IEEE Workshop on Signal Processing Advances in Wireless Communications - SPAWC 2003 (IEEE Cat. No.03EX689), 2003, pp. 190-194, doi: 10.1109/SPAWC.2003.1318948.

[12] Dupleich, R. Müller and R. Thomä, "Practical Aspects on the Noise Floor Estimation and Cut-off Margin in Channel Sounding Applications," 2021 15th European Conference on Antennas and Propagation (EuCAP), 2021, pp. 1-5, doi: 10.23919/EuCAP51087.2021.9411409.

[13] Joseph Hoellinger, Gloria Makhoul, Raffaele D'Errico Thierry Marsaul "V2V Dynamic Channel Characterization in 5G mmWave Band" International Symposium on Antennas and Propagation (ISAP) Reviewed

[14] J. Huang, C. -X. Wang, H. Chang, J. Sun and X. Gao, "Multi-Frequency Multi-Scenario Millimeter Wave MIMO Channel Measurements and Modeling for B5G Wireless Communication Systems," in IEEE Journal on Selected Areas in Communications, vol. 38, no. 9, pp. 2010-2025, Sept. 2020, doi: 10.1109/JSAC.2020.3000839.